IET Seminar on Ultra Wideband Systems, Technologies and Applications, Apr. 2006 Page(s):160 - 164

UWB Body-Centric Network: Radio Channel Characteristics and Deterministic Propagation Modelling

Y. Hao, A. Alomainy, Y. Zhao and Clive Parini

Department of Electronic Engineering, Queen Mary University of London
Mile End Road, London E1 4NS, UK
E-mail: y.hao@elec.qmul.ac.uk

Keywords: Body Area Network (BAN), Finite-Difference Time-Domain (FDTD), On-Body Channel, Ultra-Wideband (UWB).

Abstract

With the introduction of low-power, high data rate ultra wideband (UWB) technology, the idea of providing constant and reliable personal communication services with the user being the centre of attention seems more feasible and attractive. The paper presents UWB on-body radio channel characteristics in both large-scale (path loss) and small-scale (delay) prospective. Radio channel modelling using a sub-band Finite-Difference Time-Domain (FDTD) method in the frequency band 3 - 9 GHz is performed. The band is uniformly divided into 12 sub-bands in order to take into account the material frequency dispersion, each sub-band is simulated separately and then a combination technique is used to recover all simulations at the receiver. Respective modelling results from two-dimensional (2-D) and three-dimensional (3-D) sub-band FDTD models show good agreement with measurement results.

1 Introduction

Communication systems applying a user-centric approach in which services are constantly available with re-configurability, unobtrusiveness and true extension of the human's mind map the road for future revolutionary personalised networks. Current body area networks (BAN) are used to receive or transmit simple information collected from various sensors scattered around the body which requires very low processing capabilities, e.g. patient monitoring systems [1]. UWB low transmit power requirements allow longer battery life for body worn units [2]. This leads to UWB being a potential candidate for BAN. The possibility of transmitting data with various requirements in short-range communication with low-power consumption offered by UWB introduces an attractive solution for wireless BAN and implant radio system designers.

Wireless body-centric network has special properties and requirements in comparison to other available wireless networks caused by the rapid changes in communication channel behaviour on the body during the network operation. Accurate prediction of radio propagation behaviour is crucial to system design. Site measurements have the advantage of accounting for all parameters without pre-assumptions. They are, however expensive and time consuming. It is therefore necessary to develop effective propagation models for wireless system design based on generalisation of the channel characteristics. Recent UWB propagation characterisation and modelling literature has presented rigorous investigations and analysis on the behaviour of indoor UWB communication channels and transmission [3], [4].

On-body channel characterisation has been presented in a few references, e.g. [5] for narrowband channels. UWB body area network channel characterisation has been presented in few literatures [6], [7] with more realistic representation of the human body behaviour such as different body positions and postures for various antenna systems [8], [9]. Fort *et al* simulated pulse propagation around the torso at the frequency range 2 - 6 GHz using Remcom XFDTD [10]. However, the variation of UWB on-body channel at different frequencies caused by material dispersion was not taken into account. In this paper, a sub-band FDTD method is applied in order to take into account the material dispersion at different frequencies [11].

The paper presents on-body radio channel characterisation through experimental investigations with channel parameters evaluated statistically analytically. Path loss and delay channel models are introduced for different antenna types with different properties. Numerical modelling applying sub-band FDTD is used to model the on-body propagation channel with respect to different scenarios and body postures.

2 On-Body Radio Channel Characterisation

On-body UWB propagation measurement in the frequency domain using a vector network analyser is performed following the procedures described in [8], [9]. Frequency band 3 - 9 GHz, with intervals of 3.75 MHz, is chosen for the measurement. Two sets of measurements were performed in the anechoic chamber to determine the channel characteristics of various on-body links, fig.1a shows the different antenna positions placed on the body. Planar inverted cone antenna (PICA) and horn shaped self-complementary antenna (HSCA) are used. Different on-body scenarios applied in the measurements, illustrating possible body movements and potential positions of body worn devices [8], [9].

The measured channel data for the different on-body scenarios were calculated and processed in both the frequency and time domain to obtain the initial statistical parameters for both path loss and power delay profiles, including the mean excess delay spread. Their reliability and applicability are investigated against established empirical and theoretical propagation models.

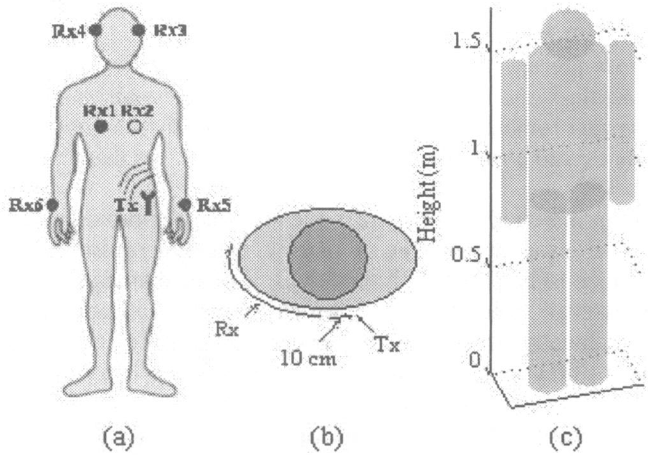

Fig. 1 Two-dimensional (2-D) and three-dimensional (3-D) human body models: (a) Antenna positions for on-body radio channel modelling and measurement (b) A 2-D ellipse cylinder used for modelling both transmitter and receiver mounted on the trunk (c) A 3-D human body model used in the sub-band FDTD model.

2.1 Large-Scale Path Loss

The path loss of the channel is calculated directly from the measurement data using averaging over the measured frequency transfers at each frequency points. It is known that the mean path loss referenced to a distance d_o (reference distance is 15 cm as calibrated for VNA measurement) can be modelled as a function of distance with least fit square used to calculate path loss exponent, γ. Figure 2 presents the measured values and modelled path loss for both antenna cases. The two types of antennas give different path loss exponents. For HSCA, $\gamma = 4.5$ and 2.8 for PICA.

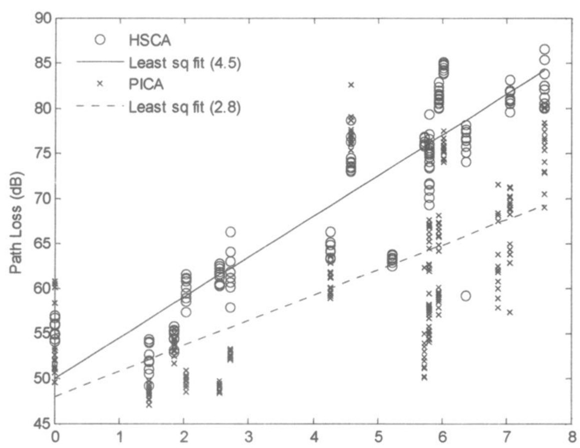

Fig. 2 Measured and modelled path loss for HSCA and PICA propagation measurements

These high exponent values are due to the non reflecting environment in the anechoic chamber. In the PICA case the modelled line is less steep than HSCA one due to multipath propagation from the human body and clothes in PICA measurement with excellent omni-directional radiation and gain across UWB range. In addition to path loss variation as a function of distance, fig.7 presents the path loss as a function of the on-body channel measurement scenario for PICA measurement.

Figure 3a shows the CDF of the deviation of the measured received power from the calculated average. The curves in general fit a normal distribution fairly good however, the PICA scenario seem to have a little more of a deviation from this distribution. These distributions present shadowing effects of the human body. The probability distribution of the signal strength is obtained from the measured data for both HSCA and PICA. The PDF of the path loss is shown in fig.3b. PDFs are approximately log normal for PICA case with scale factor of $\sigma = 0.15$. However, it is noticeable from the distribution of HSCA case that two peaks exists which can be related to body posture changes effects on link geometry and antenna radiation performance, hence dual distribution fit is applied with σ of 0.08 and 0.05.

2.2 Channel Delay Parameters

The PDP is characterised by the first central moment (mean excess delay, τ_m) and the square root of the second moment of the PDP (RMS delay spread, τ_{rms}). The RMS delay spread provides a figure of merit for estimating data rates for multipath channels. As expected, the mean delay due to the propagation link between the transmitter (Tx) and the receiver at the back (Rx2) link is the highest, where non-Line-Of-Sight (NLOS) channel and propagation around human body on the surface (creeping waves) are the main propagation channels. Figure 3 shows the cumulative distributions of the RMS delay spread for both PICA and HSCA measurements. Log Normal distribution is also plotted for each case with ($\sigma = 2.38$, $\mu = 3.5$) and ($\sigma = 2.12$, $\mu = 3.4$) for the RMS cdf of HSCA and PICA cases, respectively. Other different empirical distributions were applied, however, log normal proved to be the best fit with a larger variance for PICA channels, which is predictable due to the random behaviour of the on-body channels.

3 Numerical Modelling of On-Body Channel

Various on-body antenna positions and different body postures are applied to obtain a deterministic UWB channel model. Fig. 1a shows the transmitting and receiving antenna positions as used during measurement and modelling using a sub-band Finite-Difference Time-Domain (FDTD) method [11]. The main advantage of the sub-band FDTD method is its accuracy when modelling complicated UWB on-body radio channels since FDTD can fully account for the effects of reflection, diffraction and radiation.

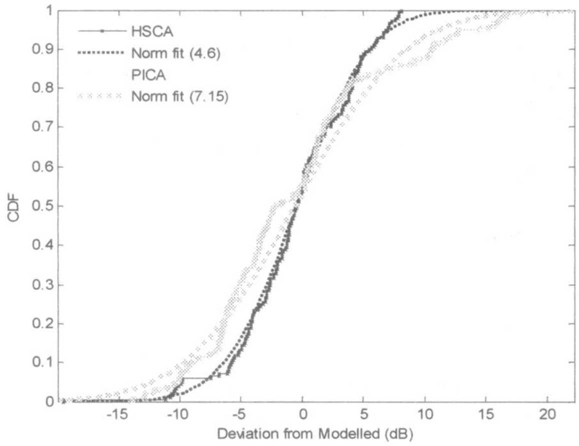

(a)

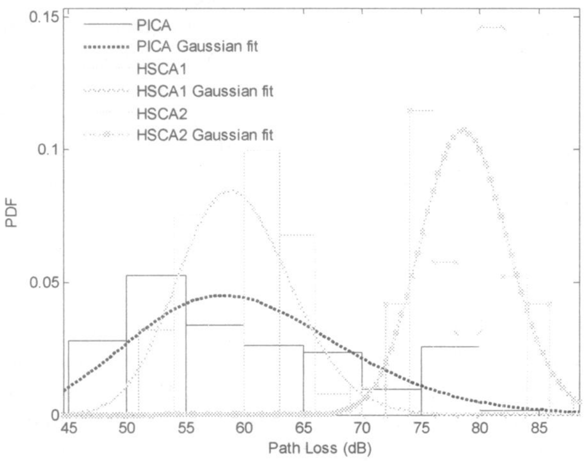

(b)

Fig. 3 (b) Deviation of measured received power from average power for both self-complementary and vertical antenna cases fitted to a normal distribution, (a) Probability distribution of measured path loss data for both vertical antenna and self-complementary antenna.

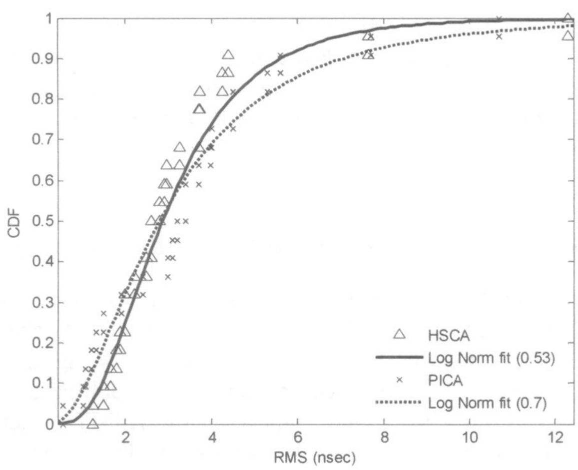

Fig. 4 Delay parameters cumulative distribution fit to log-normal distribution RMS delay spread for on-body channels

The sub-band FDTD method has been proposed in [11]. To apply the method to UWB on-body radio channel modelling, the whole frequency band (3 - 9 GHz) is first divided into 12 sub-bands with 500 MHz bandwidth for each sub-band. The choice of number of sub-bands depends on the accuracy requirement to approximate dispersive material properties. For instance, the relative dielectric constant of human muscle ranges from 52.058 at 3 GHz to 44.126 at 9 GHz [12]. 12 sub-bands are used to match the frequency dispersion curve by assuming the dielectric constant within each sub-band constant (obtained at the centre frequency of each sub-band). The overall error from such a curve fitting is less than 1%.

In the sub-band FDTD model, the antenna is approximated as a point source emitting a narrow Gaussian pulse and is deemed to be particularly viable for a vertical antenna over a horizontal ground plane, which radiates almost omni-directionally across the frequency band. Applying the sub-band FDTD method to a simple (2-D) scenario is considered. Both the transmitter and receiver are mounted on the trunk of the body. As the receiver moves along the trunk in the same horizontal plane, the scenario can be treated as a 2-D case. The human body (trunk) is modelled as a 2-D ellipse cylinder with semi-major axis 0.15 m and semi-minor axis 0.12 m according to the dimensions of a human candidate volunteer for the measurement. Both transmitter and receiver are placed on the 'trunk' and the transmitter is 10 cm offset from the centre. During the measurement, the receiver is always kept on the 'trunk' while moving along the route as shown in fig. 1b.

Only the TM-polarised field is considered for the sub-band FDTD model according to the orientation of the antenna (printed PICA) placed in measurement. The antenna pattern contribution is excluded in this analysis because, for any receiver location, the received signal only contains the contributions from two creeping waves travelling from the transmitter in opposite directions tangential to the ellipse's surface. The approximate elliptic 'trunk' is modelled with the cell size of 3.0×10^{-3} m and time step 5.0×10^{-12} s. The number of cells in the computational region is 140×160, which are truncated by a 10-cell Berenger's perfect matched layer (PML) [13].

Fig. 5 shows the path loss results along the trunk from the sub-band FDTD model and measurement. Good agreement is achieved when the creeping distance of the transmitter and receiver is small. However, when the distance approaches the maximum, variations are observed from measurement, which are caused by the adding up or cancelling of two creeping rays travelling along both sides of the elliptical 'trunk'. The sub-band FDTD model fails to accurately predict such phenomenon due to the staircase approximation of the curved surfaces and such a problem can be alleviated by using a conformal FDTD method [14].

The sub-band FDTD method is also applied to model the UWB on-body radio channel in three dimensions. As shown in fig. 1a, different antenna positions are chosen due to locations of commonly used on-body communication devices such as head mounted display, headset, and wristwatch. The human body is modelled by several different geometries: 1 sphere for the head (r = 0.10 m), 1 ellipse cylinder for the trunk (a = 0.15 m, b = 0.12 m, h = 0.65 m) and 4 cylinders for arms (r = 0.05 m, h = 0.70 m) and legs (r = 0.07 m, h = 0.85 m) according to the candidate's dimensions. The whole body is modelled as muscles and the dielectric constant and conductivity are obtained from measurement [12].

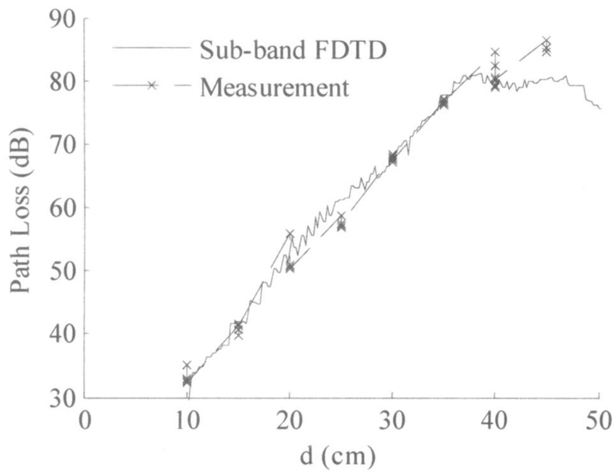

Fig. 5 Comparison of path losses along the trunk (Fig. 1b) from the sub-band FDTD model and measurement.

The human body is modelled in free space which is meshed by 140×160×630 cells with a cell size of 3.0×10^{-3} m. The time step is chosen as 5.0×10^{-12} s according to the stability criterion. The antenna over a horizontal ground plane is modelled as a point source due to its omni-directional radiation properties. The received signal at location Rx4 (fig. 1a) is shown in fig. 6.

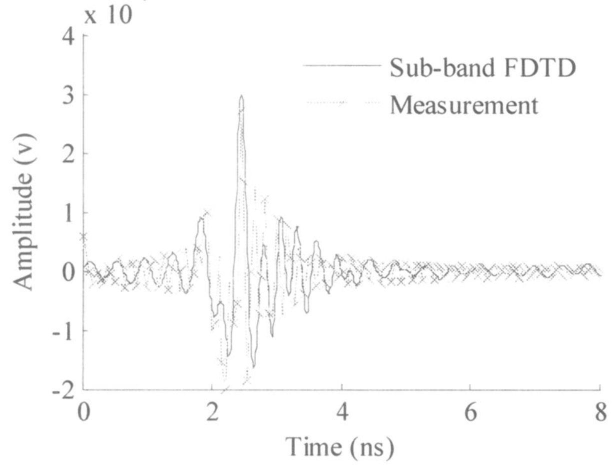

Fig. 6 Comparison of channel impulse responses at Rx4 (Fig. 1a) from the sub-band FDTD model and measurement.

It can be seen that the modelling result shows good agreement with measurement, which indicates that the approximation of PICA as a point is reasonable. However, the discrepancy is mainly due to the slight pattern distortions of PICA at different frequencies.

In the local area of each receiver (Rx1 - Rx6), two more receiver locations are considered, thus path losses at a total of 18 different locations are obtained. Then the average path loss is calculated around each receiver location and compared with measurement results, as shown in fig. 7. It can be seen that the sub-band FDTD model is capable of providing reliable modelling results for the distinctive on-body radio channel.

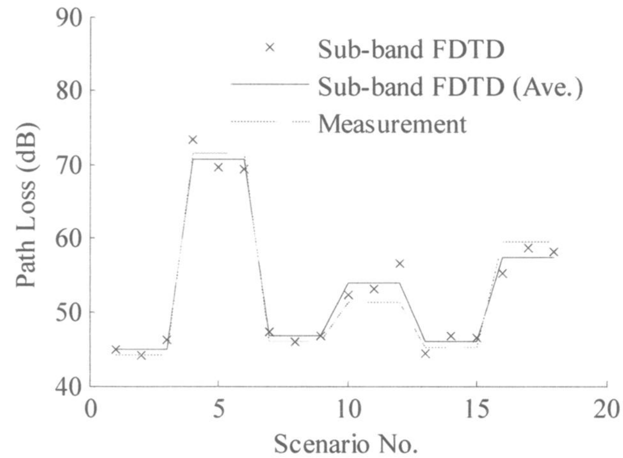

Fig. 7 Comparison of the average path loss around each receiver location for different on-body scenarios (Rx1 - Rx6, Fig. 1a).

Fig. 8 shows the comparison of modelled and measured path loss for the on-body channel. The calculated path loss exponent is also shown in the figure. The high exponent value is due to the non-reflecting environment (free space) in our models. It can be seen that the modelling results are in good agreement with measurements.

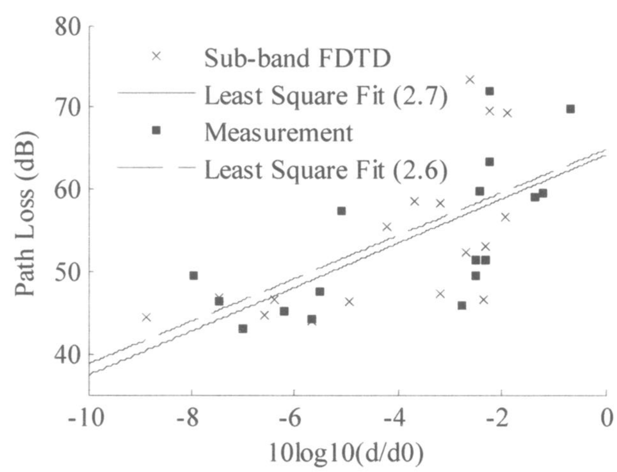

Fig. 8 Comparison of path loss for on-body channels from the sub-band FDTD model and measurement. The least square fitted lines and path loss exponent are also shown.

4 Conclusion

On-body propagation measurement with various antenna types and changes in body postures were considered. Variation in both delay parameters and path loss were observed when changes in body positions occur for all measurement scenarios. Received power was proven to be dependent not only on the antenna positions and distance but also on the frequency dependency of both antennas and on-body channel. Measured RMS spread delay fits to a log-normal distribution, which provides a tool for empirical on-body propagation modelling that can be combined with any other models representing different operating environments. The channel characteristics showed that the vertical cone antenna over a horizontal ground plane (PICA) had the best performance.

Radio channel modelling applying numerical techniques for wireless BAN communication links was discussed. The on-body propagation channel modelling using a sub-band FDTD method was presented. A combination technique is used at the receiver to recover all sub-band simulations. The advantage of this method is its ability of modelling materials with any type of frequency dependence. The sub-band FDTD method is applied to both 2-D and 3-D on-body scenarios and compared with measurement results. Good match with measured channel data is achieved.

References

[1] J. Bernardhard, P. Nagel, J. Hupp, W. Strauss, and T. von der grun, "BAN-Body area network for wearable computing," presented at 9^{th} *Wireless World Research Forum Meeting*, Zurich, Jul, 2003.

[2] J. Foerster, E. Green, S. Somayazulu and D. Leeper, "Ultra-Wideband for Short- or Medium- Range Wireless Communications", Intel technology Journal, Q2, 2001.

[3] C. Chong, Y. Kim and S. Lee, "UWB Indoor Propagation Channel Measurements and Data Analysis in Various Types of High-Rise Apartments", in *Proc.IEEE Vehicular Technology Conference (VTC2004-Fall),* Los Angeles, USA, September 2004.

[4] S. S. Ghassemzadeh, R, Jana, C. W. Rice, W. Turin and V. Tarokh, "A Statistical Path Loss Model for in-home UWB Channels", in *IEEE Conference on Ultra Wideband Systems and Technologies, UWBST,* 2002, pp. 59-64.

[5] Y. Nechayev, P. Hall, C. C. Constantinou, Y. Hao, A. Owadally and C. G. Parini, "Path Loss Measurements of On-Body Propagation Channels," in *Proc.2004 International Symposium on Antennas and Propagation*, Sendai, Japan, Aug. 2004, pp. 745- 748.

[6] I. S. Kovacs, G. Pedersen, P. Eggers and K. Olesen, "Ultra Wideband Radio Propagation in Body Area Network Scenarios", in ISSSTA Proceedings, 2004, pp: 102-106.

[7] Andrew Fort, Claude Desset, Julien Ryckaert, Philippe De Doncker, Leo Van Biesen, and Piet Wambacq, "Characterization of the ultra wideband body area propagation channel", International Conference on Ultra-WideBand, ICU'05, Zurich, Switzerland, September 2005.

[8] Alomainy, Y. Hao, X. Hu, C. G. Parini and P. S. Hall, "UWB On-Body Radio Propagation and System Modelling for Wireless Body-Centric Networks", IEE Proceedings Communications, Special Issue on UWB Theory and Technology. (To be published July 2006).

[9] Alomainy, Y. Hao, C. G. Parini and P. S. Hall, "Comparison between Two Different Antennas for UWB On-Body Propagation Measurements", IEEE Antennas and Wireless Propagation Letters, Volume 4, Issue 1, December 2005, pp: 31-34.

[10] A. Fort, C. Desset, J. Ryckaert, P. Doncker, L. Biesen and S. Donnay, "Ultra Wide-band Body Area Channel Model", 2005 IEEE International Conference on Communications, Vol. 4, 16-20 May 2005.

[11] Y. Zhao, Y. Hao and C. G. Parini, "Two Novel FDTD Based UWB Indoor Propagation Models", 2005 IEEE International Conference on Ultra-Wideband, September 5th - 8th, 2005.

[12] "An Internet Resource for the Calculation of the Dielectric Properties of Body Tissues", Institute for Applied Physics, Italian National Research Council, http://niremf.ifac.cnr.it/tissprop/.

[13] J. R. Berenger, "A Perfectly Matched Layer for the Absorption of Electromagnetic Waves," J. Computat. Phys., vol. 114, pp. 185200, Oct. 1994.

[14] Y. Hao and C. J. Railton, "Analyzing Electromagnetic Structures with curved Boundaries on Cartesian FDTD Meshes", IEEE Transactions on Microwave Theory & Techniques, Vol.46, No.1, pp.82-8, Jan. 1998.